

# Topological Entropy in Wireless Networks Subject to Composite Fading

Justin P. Coon

Department of Engineering Science  
University of Oxford  
Parks Road, Oxford OX1 3PJ, UK  
e-mail: justin.coon@eng.ox.ac.uk

Peter J. Smith

School of Mathematics and Statistics  
Victoria University of Wellington  
Cotton Building, Gate 7, Wellington, New Zealand  
e-mail: peter.smith@vuw.ac.nz

**Abstract**—We analyze topological entropy in wireless networks that are subject to local scattering and macroscopic shadowing effects. To this end, we model a network as a random geometric graph with probabilistic pair connections (due to channel randomness) and define uncertainty as the Shannon entropy of the underlying graph ensemble. We present new bounds on topological entropy that are functionals of the underlying composite fading distributions and use these to show that different fading models lead to very different network entropies under certain conditions, a result that has significant implications for self-organization and storage of the network state. We also study the behavior of the entropy bounds as the number of nodes  $n$  in the network grows large while the typical connection range  $r_0$  varies monotonically with  $n$ . This analysis leads to two key results that quantify the rate of growth or decay of  $r_0$ , as a function of the number of nodes  $n$ , that must be obeyed in order for the entropy bounds to converge to a positive limit. Although the contributions of this paper are theoretical, they have applications in systems such as ad hoc networks employing opportunistic routing and device-to-device (D2D) networks for future cellular communication.

**Index Terms**—Random geometric graphs, network topology, routing, entropy, connectivity, composite fading.

## I. INTRODUCTION

The availability of topology information at a central entity, or in a distributed nature, is of great importance in many wireless networks [1]. This information provides a view of connectivity at a fundamental level, but it can also be exploited in practice to optimize modulation, coding, and routing [2], [3]. In many wireless networks, the network topology is uncertain due to fluctuations in the channel (fading) or owing to node mobility, i.e., wireless network topologies inherently possess entropy. Network synchronization [4], route stability [5], and the conveyance of topology information throughout the network [6] are governed by the level of topological entropy in the network, and hence the quantification of this entropy is a worthwhile task.

Topological entropy has been studied in the fields of biology, chemistry, sociology, and computer science through the mathematical formalism of graph entropy [7], [8]. Mostly, research has been focused on networks and graphs whose distributions do not rely on an underlying spatial embedding, e.g., the study of the Erdős-Rényi (ER) graph formalism in database storage [9]. In contrast to these “non-spatial” network models, the topology of a wireless communication network inherently

depends upon the geometric and physical nature of the space in which it is situated, a dependence that arises through propagation effects. Topological uncertainty in dynamic mobile ad hoc networks was investigated in [6], and [10] treated self-organization of networks using a basic graph entropy framework. Recently, a more formal analysis of entropy network topologies was conducted under the assumption that the channel exhibits rich scattering characteristics (Rayleigh fading) [11].

In this paper, we develop the work reported in [11] further by treating networks that are subject to composite small-scale/large-scale fading. We approach this problem through the formalism of random geometric graphs (RGGs). Our network model accounts for random node positions and link states affected by composite fading, and uncertainty is quantified in terms of the Shannon entropy of the graph topology. We derive new bounds on topological entropy that are functionals of the underlying composite fading distributions and use these to show that different fading models lead to very different network entropies under certain conditions. We also study the behavior of the entropy bounds as the number of nodes  $n$  in the network grows large while the typical connection range  $r_0$  (to be defined later) varies monotonically with  $n$ , and provide two key lemmas that quantify the rate of growth or decay of  $r_0$ , as a function of the number of nodes  $n$ , that must be obeyed in order for the entropy bounds to converge to a positive limit. These results help us to understand how system parameters such as transmit power affect disorder in large-scale networks (through  $r_0$ ), and point to design guidelines that are useful for controlling topological uncertainty in practice. Although the contributions of this paper are largely theoretical, readers with a grounding in basic information theory will recognize that topological entropy represents the amount of information that a graph ensemble embodies. As a result, the study of this quantity has implications for self-organization, storage of the network state, calculation of routing tables, and the communication of network topology information through a network.

The rest of the paper is organized as follows. In section II, we give details of the network, pair connection model, and definitions of entropy considered in this work. We investigate topological entropy for networks subject to composite fading in section III. Sections IV and V provide details of bounds on

topological entropy for small and large typical pair connection ranges, and treat specific questions of RGG entropy as the number of nodes in the network grows while the typical connection range for each node varies monotonically with  $n$ . Conclusions are given in section VI.

*Notation:* The expectation operation is denoted by  $\mathbb{E}[\cdot]$ .  $\mathbb{I}(\cdot)$  is the indicator function, which is equal to one if the argument is true and zero otherwise.  $\Gamma(a) = \int_0^\infty t^{a-1} e^{-t} dt$  is the gamma function. For nonnegative functions  $f(n)$  and  $g(n)$ , the notation  $f(n) = O(g(n))$  signifies that for some  $k_0 > 0$ , there exists an  $n_0 > 0$  such that  $f(n) \leq k_0 g(n)$  for all  $n > n_0$ .

## II. SYSTEM MODEL AND GRAPH ENTROPY

### A. Network Model

Consider a set of  $n$  nodes (wireless devices)  $\mathcal{V}$  embedded in  $\mathcal{K}_d \subset \mathbb{R}^d$ , which has volume  $K_d = |\mathcal{K}_d|$ . The locations of the nodes, denoted by  $\mathbf{r}_1, \dots, \mathbf{r}_n$ , are modeled as a binomial point process (BPP) in  $\mathcal{K}_d$ . We use the index  $i$  and the location  $\mathbf{r}_i$  interchangeably to refer to node  $i$ . It is important to note that, in general, the BPP is not restricted to be homogeneous. Furthermore, other point processes (e.g., Poisson) could be easily considered without significantly altering the basic analytical framework presented below.

We model a wireless network as an instantiation of an undirected RGG. We denote the ensemble of graphs by  $\mathcal{G}$ , and each graph  $g \in \mathcal{G}$  is described by the node set  $\mathcal{V}$ , the particular embedding mentioned above, and the resulting edge set  $\mathcal{E}_g$ , where each edge represents a directly established communication link between two nodes in the network. An edge  $(i, j)$  exists between nodes  $i$  and  $j$ , separated by a (Euclidean) distance  $r_{i,j} = \|\mathbf{r}_i - \mathbf{r}_j\|$ , with probability  $p(r_{i,j}) := p_{i,j}$ .

### B. Composite Fading Model

We call the probability  $p_{i,j}$  the *pair connection function* for nodes  $i$  and  $j$ . Allowing edges to exist probabilistically will enable us to consider the effects that large-scale and small-scale fading have on the network topology. Note that previous works have generally only considered hard disk pair connection functions, i.e.,  $p(r) = \mathbb{I}(r \leq r_0)$  for  $r_0 > 0$  [10], or completely different random graph formalisms [9].

In the most general case, the propagation model should account for small-scale fading, which arises from multipath propagation in rich scattering environments, as well as large-scale fading (shadowing), which typically results from macroscopic blockages. Thus, the pair connection function can logically be defined as the complement of the outage probability  $\mathbb{P}(\text{SNR}(r) > t)$  where

$$\text{SNR}(r) \propto \frac{XY}{r^\eta}. \quad (1)$$

Here,  $\eta$  is the path loss exponent, and  $X$  and  $Y$  are random variables denoting the small-scale and large-scale channel gains, respectively. For example, for the case where small-scale Rayleigh fading is assumed,  $X$  would be exponentially distributed. Analogously, if the popular log-normal shadowing model is assumed,  $Y$  would follow a log-normal distribution.

We do not specify such distributions at present in order to maintain generality. This approach will later enable us to derive general bounds on the topological entropy that depend only on relatively simple statistics of the channel, irrespective of the exact underlying fading models. Under the assumptions stated above, we can write the pair connection function as

$$p(r) = \mathbb{P}(XY > (r/r_0)^\eta) \quad (2)$$

where  $r_0$ , which is related to the proportionality constant in (1), is the *typical connection range*. This parameter is usually defined by system variables including the transmission frequency, antenna gains, and the noise figure associated with the receiver amplifiers; hence, although it appears to be unphysical, it actually encompasses most system parameters that have engineering importance (see, e.g., [12]). Note that by letting  $\eta \rightarrow \infty$ , we recover the hard disk connection function with radius  $r_0$ . This generality provides further motivation for defining the constant  $r_0$  in the manner stated above.

### C. Graph Entropy

We quantify topological entropy in the context of wireless networks by studying the Shannon entropy of the underlying RGG ensemble. The entropy of a graph  $G$  can be written as<sup>1</sup>

$$H(G) = \mathbb{E}[-\log_2 \mathbb{P}(G)] = - \sum_{g \in \mathcal{G}} \mathbb{P}(g) \log_2 \mathbb{P}(g). \quad (3)$$

The exact expression for  $H(G)$  appears to be intractable in bounded domains due to edge dependence that arises from the spatial embedding. However, the following simple, but useful, upper bound was derived in [11]:

$$\bar{H}_n := \binom{n}{2} H_2(\bar{p}) \geq H(G) \quad (4)$$

where

$$\bar{p} = \int_0^D p(r) f(r) dr \quad (5)$$

and

$$H_2(\bar{p}) = -\bar{p} \log \bar{p} - (1 - \bar{p}) \log(1 - \bar{p}) \quad (6)$$

is the binary entropy function. In (5),  $f(r)$  is the pair distance density corresponding to a BPP in  $\mathcal{K}_d$ , and  $D = \sup_{\mathbf{r}_i, \mathbf{r}_j \in \mathcal{K}_d} \|\mathbf{r}_i - \mathbf{r}_j\|$  is the diameter of the domain. Hence, (5) signifies the *average* pair connection probability in  $\mathcal{K}_d$ .

## III. EFFECTS OF COMPOSITE FADING ON ENTROPY

The bound on entropy given in (4) is a functional of the pair distance density  $f(r)$  and the pair connection probability  $p(r)$ . The geometry of the domain  $\mathcal{K}_d$  defines  $f(r)$ . Analytic expressions for  $f(r)$  exist for homogeneous BPPs in simple convex domains (e.g., circles or squares in  $\mathbb{R}^2$ ). For more complicated configurations,  $f(r)$  can be estimated empirically through Monte Carlo simulations. Although the exact form of  $f(r)$  may be of interest in certain applications, such as random

<sup>1</sup>Here, capital  $G$  denotes a random variable. Lowercase  $g$  will be reserved for particular elements of the ensemble  $\mathcal{G}$ .

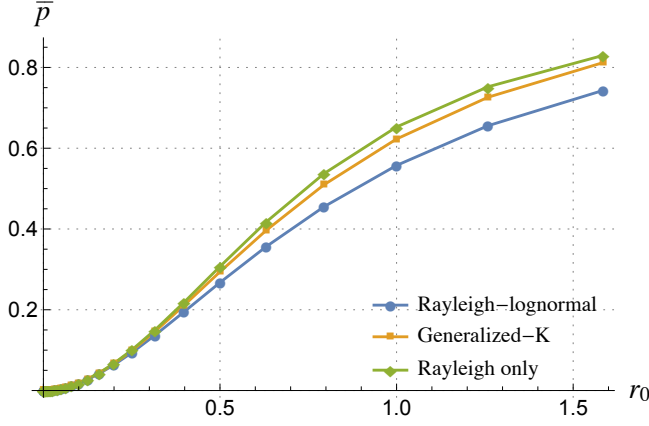


Fig. 1. Average pair connection probability for different composite fading models. The statistical parameters were chosen such that the mean channel gain for each model is 2: Rayleigh-lognormal ( $\mu_x = 1, \mu_y = \ln 2/2, \sigma_y = \sqrt{\ln 2}$ ); generalized-K ( $m_m = 1.5, m_s = 2, \Omega_0 = 2$ ); Rayleigh only (exponential with a mean of 2). The network domain is a circle of radius one, and  $\eta = 2$ .

sensor network deployments in a given closed domain, we will focus on the pair connection function  $p(r)$  here. Hence, to make progress, we will mostly consider the case where the network is confined to a circle (in  $\mathbb{R}^2$ ) of radius  $R$ . For a homogeneous BPP in a circle, we have [13]

$$f(r) = \frac{2r}{R^2} - \frac{r^2}{\pi R^4} \sqrt{4R^2 - r^2} - \frac{4r}{\pi R^2} \sin^{-1}(r/2R). \quad (7)$$

For the interested reader, expressions for other spherical domains can be found in [13], [14] gives distributions for regular polygons, and [15] details a general theory of distance statistics.

Under a composite fading assumption, we may adopt a number of potential models for the pair connection function  $p(r)$ . Canonical models are based on Rayleigh-lognormal compositions [16], [17]. Tractability poses a problem in these cases, so researchers have also proposed other models, such as the generalized-K distribution [18] and moment-matched gamma distributions [19]. For our study of graph entropy, any of these models can be adopted in principle, but we will focus on the Rayleigh-lognormal and generalized-K models, specifically, in order to provide a useful comparison. Letting  $\rho(r) = (r/r_0)^\eta$  for brevity, we can write the pair connection function for the Rayleigh-lognormal model as [20]

$$p(r) = \int_0^\infty \frac{1}{\sqrt{2\pi}y\sigma_y} \exp\left(-\frac{\rho(r)}{\mu_x y} - \frac{(\log y - \mu_y)^2}{2\sigma_y^2}\right) dy \quad (8)$$

where  $\mu_x = \mathbb{E}[X]$ , and  $\mu_y$  and  $\sigma_y$  are the lognormal parameters that satisfy  $\mathbb{E}[Y] = e^{\mu_y + \sigma_y^2/2}$  and yield a median value for  $Y$  equal to  $e^{\mu_y}$ . For the generalized-K model, we have

$$p(r) = 1 - \pi \csc(\pi\beta) \frac{\omega(r)^{m_m} {}_1F_2(m_m; m_m + 1, 1 - \beta; \omega(r))}{\Gamma(m_m + 1)\Gamma(m_s)\Gamma(1 - \beta)} + \pi \csc(\pi\beta) \frac{\omega(r)^{m_s} {}_1F_2(m_s; m_s + 1, 1 + \beta; \omega(r))}{\Gamma(m_m)\Gamma(m_s + 1)\Gamma(1 + \beta)} \quad (9)$$

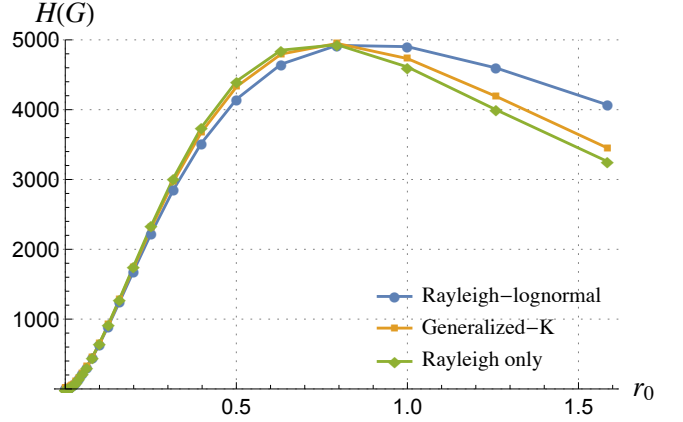


Fig. 2. Entropy bound (4) measured in bits for a network of 100 nodes in a unit circle with different composite fading models. The statistical parameters for the different models are the same as in Fig. 1.

for  $m_m \geq 1/2$  and  $m_s > 0$  [19]. Here, the notation  ${}_pF_q(a_1, \dots, a_p; b_1, \dots, b_q; z)$  represents the generalized hypergeometric function,  $\beta = m_s - m_m$ ,  $\omega(r) = m_m m_s \rho(r) / \Omega_0$ ,  $m_m$  and  $m_s$  are the shape factors of the underlying gamma distributions that the generalized-K distribution is derived from, and  $\Omega_0$  is the scale parameter (see [19]).

To calculate the mean pair connection function, the appropriate distribution function (e.g., (8) or (9)) would simply need to be substituted into (5), along with (7) or another suitable pair distance density, and the integral evaluated numerically. This has been done to produce Fig. 1. It is observed in this figure that different fading models lead to significant variations in  $\bar{p}$ , especially for large typical connection ranges. Substituting these values for  $\bar{p}$  into (4) gives the entropy bounds plotted in Fig. 2. The discrepancies between different models are even more striking in this example, and one can easily draw conclusions about the importance of basing these calculations on an accurate model for a particular application. Indeed, for  $r_0 = 1.6$ , the Rayleigh-lognormal model suggests that about 4,000 bits are needed to store the network topology compared to the 3,500 bits needed to store the same information if the fading environment more closely resembles a generalized-K model.

Fig. 2 illustrates a few other salient features that are of interest from both a theoretical and a practical perspective. In particular, the entropy bounds are unimodal in the typical connection range. This implies that, in practice, uncertainty can be tuned by adjusting the transmit powers of the devices. Network engineers may wish to control entropy in this way to limit the amount of storage that is needed to encompass the topology information, or to constrain the length of the required bit field in the routing table. It can also be inferred from Fig. 2 that the topological entropy decays to zero in the limits of large or small  $r_0$ . Intuitively, this makes sense, because one would expect a disconnected network with near certainty if  $r_0 \simeq 0$ , or a completely connected network when  $r_0 \gg D$ .

#### IV. ANALYTIC RESULTS FOR SMALL CONNECTION RANGES

Motivated by the observations made in relation to Fig. 2, we now analyze topological entropy in the small typical connection range regime. Based on this analysis, we will develop scaling laws that link  $r_0$  and the number of nodes in the network  $n$  to the entropy bound  $\bar{H}_n$  as  $n \rightarrow \infty$ .

##### A. Upper Bounds on Pair Connection and Entropy

In some special cases,  $\bar{p}$  can be calculated in closed form<sup>2</sup>. However, this is generally not possible when composite fading is assumed due to the complicated form of  $p(r)$ . Hence, it is beneficial to derive bounds on  $\bar{p}$ , and ultimately  $H(G)$ . For small typical connection ranges ( $r_0 \simeq 0$ ), we can bound the tail probability  $p(r)$ . Composite fading distributions are typically heavy tailed, i.e.,

$$\lim_{z \rightarrow \infty} e^{\lambda z} \mathbb{P}(XY > z) = \infty, \quad \lambda > 0. \quad (10)$$

As a direct consequence, the moment generating function of  $XY$  does not exist in general, and we cannot employ a Chernoff bound. Hence,  $p(r)$  *does not* decay exponentially, and the simple approximation used in [11, eqs. (20), (21)] cannot be used. Instead, we use the following Markov-like inequality.

$$\begin{aligned} p(r) &= \mathbb{P}(XY > \rho(r)) \\ &= \mathbb{P}((XY + \xi)^\alpha > (\rho(r) + \xi)^\alpha), \quad \alpha, \xi > 0 \\ &\leq \inf_{\alpha, \xi > 0} \frac{\mathbb{E}[(XY + \xi)^\alpha]}{(\rho(r) + \xi)^\alpha} \end{aligned} \quad (11)$$

The corresponding bound on  $\bar{p}$  is

$$\bar{p} \leq \int_0^D f(r) \inf_{\alpha, \xi > 0} \frac{\mathbb{E}[(XY + \xi)^\alpha]}{(\rho(r) + \xi)^\alpha} dr. \quad (12)$$

Note that for every  $r$  in the integrand, the minimization results in particular values of  $\alpha$  and  $\xi$ . Additionally, the expectation will typically not have a closed form. As a consequence of these issues, the calculation of the bound in (12) is generally impractical, and it does not provide much insight into how entropy depends on various statistical parameters.

A more analytically useful, but looser, bound can be obtained by choosing  $\alpha$  and  $\xi$  independently of  $r$  and  $r_0$ . This yields

$$\bar{p} \leq \inf_{\alpha, \xi > 0} \mathbb{E}[(XY + \xi)^\alpha] \int_0^D \frac{f(r)}{(\rho(r) + \xi)^\alpha} dr. \quad (13)$$

We see from this expression that the parameter  $\xi$  ensures the integral converges for all  $\alpha > 0$ . Eq. (13) admits a more useful (semi-)analytic form for standard composite fading models.

Before considering specific composite models, we note that the integral evaluates to the following general form for  $\eta = 2$

<sup>2</sup>For a pair connection function derived from a small-scale Rayleigh fading assumption only,  $\bar{p}$  can be written in terms of incomplete gamma functions for a homogeneous BPP in a 3D spherical domain, but a closed-form expression for even the 2D case is elusive.

and a circular domain of radius  $R$ :

$$\begin{aligned} \int_0^D \frac{f(r)}{(\rho(r) + \xi)^\alpha} dr &= \frac{r_0^2 \xi^{1-\alpha}}{2(\alpha-2)(\alpha-1)^2 R^2 \zeta} \left( 2(\alpha-2)(\alpha-1)\zeta \right. \\ &\quad \left. + (\zeta+1)(2\alpha(\zeta+1) - \zeta - 2) {}_2F_1\left(\frac{1}{2}, \alpha; 1; -\zeta\right) \right. \\ &\quad \left. - (2\alpha + \zeta - 2) {}_2F_1\left(-\frac{1}{2}, \alpha; 1; -\zeta\right) \right) \end{aligned} \quad (14)$$

where  $\zeta = 4R^2/r_0^2\xi$  and  ${}_2F_1(a, b; c; z)$  is the Gauss hypergeometric function. For  $\eta = 4$ , we have the analogous result

$$\begin{aligned} \int_0^D \frac{f(r)}{(\rho(r) + \xi)^\alpha} dr &= \frac{2}{\xi^\alpha} {}_4F_3\left(\frac{1}{2}, \frac{3}{4}, \frac{5}{4}, \alpha; 1, \frac{3}{2}, \frac{3}{2}; -\frac{16R^4}{\xi r_0^4}\right) \\ &\quad - \frac{1}{\xi^\alpha} {}_3F_2\left(\frac{3}{4}, \frac{5}{4}, \alpha; \frac{3}{2}, 2; -\frac{16R^4}{\xi r_0^4}\right). \end{aligned} \quad (15)$$

Closed-form results are available for other integer values of  $\eta$ , and these are typically written in terms of  ${}_pF_q$  functions. In the interest of brevity, however, we omit these expressions.

1) *Rayleigh-Lognormal*: For the Rayleigh-lognormal model, the expectation  $\mathbb{E}[(XY + \xi)^\alpha]$  does not have a simple closed form unless  $\alpha$  is a nonnegative integer, in which case we have

$$\mathbb{E}[(XY + \xi)^\alpha] = \sum_{k=0}^{\alpha} \binom{\alpha}{k} k! \xi^{\alpha-k} \mu_x^k e^{k\mu_y + \frac{1}{2}k^2\sigma_y^2}. \quad (16)$$

However, numerical investigations have shown that constraining  $\alpha$  to be a positive integer does not significantly affect the tightness of the bound given in (13), and in fact  $\alpha = 2$  approximately yields the infimum for scenarios of interest (see, e.g., Fig. 3). For this special case and when  $\eta = 2$ , the integral in (14) simplifies considerably and the expectation can be evaluated to give the bound

$$\bar{p} \leq \inf_{\xi > 0} \frac{2r_0^2 \left( 2\mu_x^2 e^{2\mu_y + 2\sigma_y^2} + 2\mu_x \xi e^{\mu_y + \frac{\sigma_y^2}{2}} + \xi^2 \right)}{\xi \left( r_0 \left( \sqrt{\xi(4R^2 + r_0^2\xi)} + r_0\xi \right) + 2R^2 \right)} \quad (17)$$

with the term inside the parentheses in the numerator denoting the contribution from the expectation to the bound (cf. (16)). This expression is plotted in Fig. 3 along with the corresponding bounds for  $\alpha = 1$  and  $\alpha = 3$ , the exact (numerically evaluated) quantity derived using (5), (7), and (8), and the approximation obtained using the method of [11]. Clearly, the approximation based on [11] is unsuitable for use with the Rayleigh-lognormal model, as indicated earlier. In contrast, the bound for  $\alpha = 2$  exhibits the same logarithmic slope, and hence converges asymptotically to the true value.

Ultimately, we wish to apply the bound given above to analyze the topological entropy of the network ensemble. Since the entropy bound  $\bar{H}_n$  is increasing for  $0 \leq \bar{p} \leq 0.5$ , we

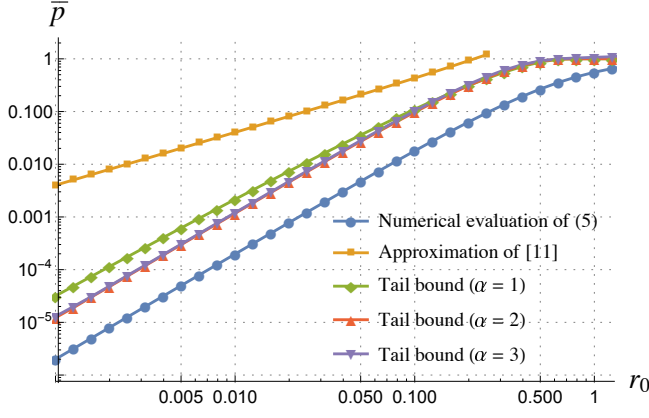


Fig. 3. Rayleigh-lognormal model: average pair connection probability bounds for different  $\alpha$  (cf. (13)). The exact (numerical evaluated) function and the approximation based on the method detailed in [11] are also shown. The statistical parameters are the same as in Fig. 1.

can apply the tail bound approach outlined here to obtain an analytic estimate for this bound for small  $r_0$ . As  $r_0$  increases, however,  $\bar{p}$  will become greater than 0.5 (cf. Fig. 3) and the bound will no longer be valid. Fig. 4 illustrates the numerically evaluated upper bound in (4), the approximation from [11], and the tail bound derived by substituting (17) into (4) for a 100 node network confined to a circle of unit radius in  $\mathbb{R}^2$ . Clearly, the logarithmic trend of the tail bound agrees with (4), thus making it useful for discerning or predicting order in large-scale applications with small connection ranges, such as battery-powered sensor networks.

2) *Generalized-K*: For the generalized-K model with non-negative integer  $\alpha$ , the expectation  $\mathbb{E}[(XY + \xi)^\alpha]$  is

$$\mathbb{E}[(XY + \xi)^\alpha] = \sum_{k=0}^{\alpha} \binom{\alpha}{k} \xi^{\alpha-k} \left( \frac{\Omega_0}{m_m m_s} \right)^k \frac{\Gamma(m_m + k) \Gamma(m_s + k)}{\Gamma(m_m) \Gamma(m_s)}. \quad (18)$$

Applying a similar approach as for the Rayleigh-lognormal case, we can use (18) and (14) to arrive at an expression for the bound that is similar to (17). The resulting estimates for the average pair connection probability and the entropy are similar to the Rayleigh-lognormal results. Hence, we omit these here.

3) *Other Models*: We may also perform a similar analysis to that presented above for different path loss exponents and different composite fading models. The methodology is the same, and the results would be analogous to those presented above. Again, due to space limitations, we refrain from including further discussion of other models here.

### B. Entropy Scaling Limit

One may wish to determine an expression for the typical connection range, as a function of the number of nodes  $n$ , that yields a positive value of  $\bar{H}_n$  as  $n \rightarrow \infty$ . Such an expression would enable us to understand how the typical connection range affects disorder in large-scale networks, and

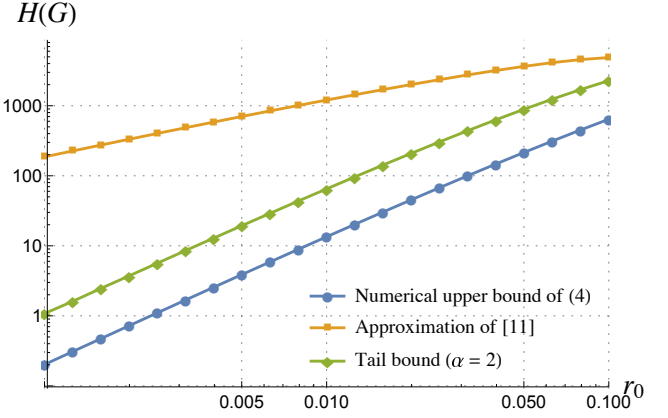


Fig. 4. Rayleigh-lognormal model: entropy bounds for a 100 node network. The numerically evaluated bound of (4), the approximation from [11], and the tail bound corresponding to (17) are shown. The statistical parameters are the same as in Fig. 1.

would point to design guidelines that are useful for controlling topological entropy in practice. Conversely, it would also yield conditions that lead to zero entropy and unbounded entropy in complex communication networks. The zero-entropy condition implies either full or no connectivity in the network with probability one (cf. Fig. 2); whereas the unbounded-entropy condition relates to potentially unpredictable network behavior as  $n$  scales. These considerations may seem to be of theoretical interest only. However, since the typical connection range is a function of the transmit power and other system parameters, we can glean insight from such an exercise that may help engineers to better understand large-scale networks.

Before proceeding, note that in (13), only the integral is a function of  $r_0$ , and this integral captures only geometric aspects of the system rather than the fading statistics. Hence, we can study the small  $r_0$  behaviour of entropy without specifying the composite fading model. The following lemma gives the relation between  $r_0$  and  $n$  that yields a fixed, positive topological entropy in the large  $n$  limit.

*Lemma 1*: The entropy bound obtained by substituting (13) into (4) will tend to a limit  $\bar{H}_n \rightarrow \ell_h > 0$  as  $n \rightarrow \infty$  and  $r_0 \rightarrow 0$  if

$$r_0(n) = \left( \frac{\varpi(n)}{C_\eta \mathbb{E}[(XY + \xi)^\alpha]} \right)^{\frac{1}{2}} \quad (19)$$

where

$$\varpi(n) = \exp \left( W_m \left( -\frac{2\ell_h}{n(n-1)} \right) \right) \quad (20)$$

with  $W_m(x)$  denoting the lower branch ( $-1/e \leq x < 0$  and  $W_m \leq -1$ ) of the solution to  $x = We^W$ . For  $\eta = 2, 4$ , the constant  $C_\eta$  is given by

$$C_2 = \frac{1}{\xi R^2} \quad (21)$$

and

$$C_4 = \frac{2\sqrt{2}\pi - \Gamma(\frac{1}{4})\Gamma(\frac{3}{4})}{4\sqrt{2}\xi^{3/2}R^2} \simeq \frac{0.7854}{\xi^{3/2}R^2} \quad (22)$$

respectively.

*Proof:* The proof follows by substituting (17) into (4), equating  $\bar{H}_n = \ell_h$ , and solving for  $r_0$  when only the leading order of (4) is retained.  $\square$

Several interesting observations can be made from this lemma. First, the scaling behavior is independent of the path loss exponent, which only affects the constant  $C_\eta$ . Since the square root of  $\varpi(n)$  decays like  $O(1/(n\sqrt{\log n}))$  [21], we see that by scaling the connection range  $r_0$  in this manner as  $n$  grows large, the uncertainty in the network topology stabilizes. One might consider a simple path loss model [22] to put some meaning to this scaling, in which case it is straightforward to show that  $r_0 \propto P_T^{1/\eta}$  where  $P_T$  is the transmit power of each node. Hence, to achieve stability in uncertainty in the limit of large  $n$ , the transmit power must scale like

$$P_T \propto (n^2 \log n)^{-\frac{\eta}{2}}. \quad (23)$$

Another interesting point to touch upon is that the scaling behavior is independent of the specific composite fading model that is assumed. Moreover, a similar scaling limit was shown in [11] for the case where small-scale Rayleigh fading only is assumed. Thus, for the small  $r_0$  limit, small-scale and large-scale fading exhibit similar scaling trends. This result can be inferred somewhat from Fig. 2, but we have backed up this observation here by concrete quantitative analysis.

## V. ANALYTIC RESULTS FOR LARGE CONNECTION RANGES

We now turn our attention to the regime where the typical connection range is large compared to the diameter of the circle domain, i.e.,  $r_0 \gg 2R$ . Here, we derive analogous results to those presented above for the small  $r_0$  case.

### A. Bounds on Pair Connection and Entropy

We can obtain a simple but useful approximation to  $\bar{p}$  by expanding  $p(r)$  for large  $r_0$ , retaining the first two terms, and finally integrating according to (5). This is possible, in principle, for any composite fading model, and we will show results for the Rayleigh-lognormal and generalized-K models below. But first, to illustrate the calculations, we provide details for the canonical case.

Consider (8), and expand for large  $r_0$ . In this case,  $\rho(r) \simeq 0$ , and the first exponential<sup>3</sup> can be approximated by

$$\exp\left(-\frac{\rho(r)}{\mu_x y}\right) \simeq 1 - \frac{\rho(r)}{\mu_x y}. \quad (24)$$

In fact, this is a lower bound for large  $r_0$  since  $e^{-x} > 1 - x$  for  $x < 1$  in general. Hence, this approach will eventually lead to an upper bound on entropy<sup>4</sup>. Substituting the approximation above into (8) and evaluating the integral, we arrive at

$$p(r) > 1 - \frac{\rho(r)}{\mu_x} e^{-\mu_y + \sigma_y^2/2}. \quad (25)$$

<sup>3</sup>Here, we take the trivial step of separating the exponential (shown in (8)) of the sum of two arguments into a product of exponentials.

<sup>4</sup>The upper bound results from the fact that  $\bar{H}_n$  decreases with  $\bar{p}$  for  $\bar{p} > 0.5$ , which is the case when  $r_0$  is large.

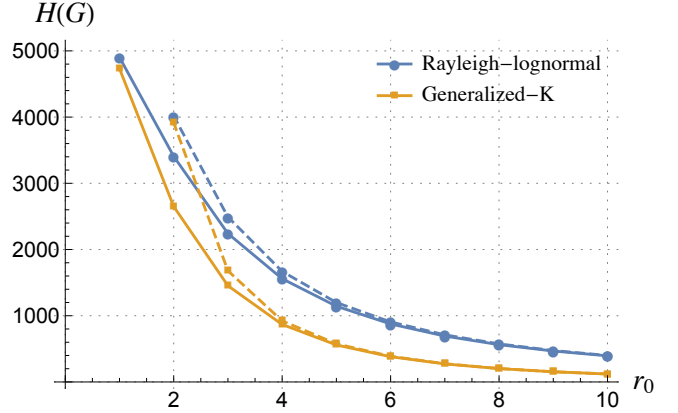


Fig. 5. Entropy bounds for a 100 node network at large  $r_0$ . Solid lines correspond to the numerically evaluated bound of (4), and dashed lines correspond to the approach detailed in section V-A are shown. The statistical parameters are the same as in Fig. 1.

Now, substituting this into (5) leads to the bound

$$\bar{p} > 1 - \frac{2e^{-\mu_y + \sigma_y^2/2} \Gamma(\eta + 3)}{\mu_x (\eta + 2) \Gamma(\frac{\eta}{2} + 2) \Gamma(\frac{\eta}{2} + 3)} \left(\frac{R}{r_0}\right)^\eta. \quad (26)$$

As noted above, this lower bound on  $\bar{p}$  gives an upper bound on  $H(G)$  for large  $r_0$  when substituted into (4). This relationship is exhibited in Fig. 5, which illustrates the entropy of a 100 node network (measured in bits) for the Rayleigh-lognormal and generalized-K composite fading models. The tightness of the approximation as  $r_0$  grows large is apparent in this example for both fading distributions. There is also a clear discrepancy between the entropies of the two cases, which again highlights the importance of correctly choosing the most representative composite fading model in practice.

### B. Entropy Scaling Limit

As with the small  $r_0$  limit, it is possible to determine an expression for the typical connection range, as a function of the number of nodes  $n$ , that yields a positive value of the entropy bound as  $r_0, n \rightarrow \infty$ . Rather than focusing on a specific fading model, we maintain generality here. The following lemma captures the relationship between  $r_0$  and  $n$  that yields a fixed, positive topological entropy in the large  $r_0$  and  $n$  limits.

**Lemma 2:** The entropy bound (4) will tend to a limit  $\bar{H}_n \rightarrow \ell_h > 0$  as  $r_0, n \rightarrow \infty$  if

$$r_0(n) = \left( \frac{|p_\rho(0)| \mathbb{E}[r^\eta]}{\varpi(n)} \right)^{\frac{1}{\eta}} \quad (27)$$

where the expectation is taken over the pair distance distribution,  $p_\rho(0)$  denotes the partial derivative of  $p(r)$  taken with respect to  $\rho$  and evaluated at zero (cf. (2)), and  $\varpi(n)$  is defined in (20). For the disk domain of radius  $R$  in  $\mathbb{R}^2$ ,

$$\mathbb{E}[r^\eta] = \frac{2\Gamma(\eta + 3)R^\eta}{(\eta + 2)\Gamma(\frac{\eta}{2} + 3)\Gamma(\frac{\eta + 4}{2})}. \quad (28)$$

*Proof:* The proof is similar that of to Lemma 1.  $\square$



The function  $\varpi(n)^{-1/\eta}$  increases like  $O((n^2 \log n)^{1/\eta})$  [21]. Thus, we see that the uncertainty in the network topology stabilizes in the limit of large  $n$  if the typical connection range *increases*. This may seem counterintuitive, but consider the alternative. Suppose a node is added to the network while keeping  $r_0$  fixed. There will be roughly  $n$  extra links that could be formed by the addition of this node, and the existence (or not) of each link is random. Thus, uncertainty increases like  $O(n^2)$ , as indicated in (4). But if we allow the connection range to *increase* with each additional node that joins the network, the likelihood of each of the (roughly)  $n$  possible extra links being established increases as well, and the link entropy  $H_2(\bar{p})$  decreases. This balances the uncertainty, and Lemma 2 quantifies this effect.

It is also interesting to note the role that the path loss exponent takes in this scaling law. In the small  $r_0$  limit, the path loss exponent manifested in the denominator of (19), and thus  $\eta$  did not affect the scaling behavior of topological uncertainty. In the case of large  $r_0$ , however,  $\eta$  has an algebraic effect on the connection range scaling rate, specifically  $O((n^2 \log n)^{1/\eta})$  as noted above. Since  $r_0 \propto P_T^{1/\eta}$ , this implies that transmit power scaling is independent of the path loss decay rate in this scenario. This phenomenon was also illuminated in [11] for the case where small-scale Rayleigh fading only is assumed.

## VI. CONCLUSIONS

In this paper, we analyzed topological entropy in wireless networks using an RGG formalism with soft pair connection functions based on composite fading distributions. We derived new bounds on RGG entropy and showed that the typical connection range must decay like  $O(1/(n^2 \log n)^{1/2})$  for the bounds to converge to a limit when the network is confined to a circle in  $\mathbb{R}^2$ . Furthermore, we analyzed the large typical connection range regime and proved that  $r_0$  must increase like  $O((n^2 \log n)^{1/\eta})$  to yield a similar limit. The results presented in this paper have significant implications for self-organization, storing and communicating network topology information, and calculating routing tables. Hence, the perspective provided by the entropy framework can be useful for designing opportunistic routing protocols and understanding the amount of control overhead needed to maintain network connectivity.

## ACKNOWLEDGMENT

This work was supported by EPSRC grant number EP/N002350/1 (“Spatially Embedded Networks”).

## REFERENCES

[1] L. Wei, R. Hu, Y. Qian, and G. Wu, “Enable device-to-device communications underlying cellular networks: challenges and research aspects,” *IEEE Commun. Mag.*, vol. 52, no. 6, pp. 90–96, 2014.

[2] L. Pelusi, A. Passarella, and M. Conti, “Opportunistic networking: data forwarding in disconnected mobile ad hoc networks,” *IEEE Commun. Mag.*, vol. 44, no. 11, pp. 134–141, 2006.

[3] T. Kathiravelu, N. Ranasinghe, and A. Pears, “Towards designing a routing protocol for opportunistic networks,” in *Advances in ICT for Emerging Regions (ICTer), 2010 International Conference on*. IEEE, 2010, pp. 56–61.

[4] D. Han and G. Chesi, “Robust synchronization via homogeneous parameter-dependent polynomial contraction matrix,” *IEEE Trans. Circuits Syst. I*, vol. 61, no. 10, pp. 2931–2940, 2014.

[5] B. An and S. Papavassiliou, “An entropy-based model for supporting and evaluating route stability in mobile ad hoc wireless networks,” *IEEE Commun. Lett.*, vol. 6, no. 8, pp. 328–330, 2002.

[6] R. Timo, K. Blackmore, and L. Hanlen, “On entropy measures for dynamic network topologies: Limits to MANET,” in *Communications Theory Workshop, 2005. Proceedings. 6th Australian*. IEEE, 2005, pp. 95–101.

[7] G. Simonyi, “Graph entropy: a survey,” *Combinatorial Optimization*, vol. 20, pp. 399–441, 1995.

[8] M. Dehmer and A. Mowshowitz, “A history of graph entropy measures,” *Information Sciences*, vol. 181, no. 1, pp. 57–78, 2011.

[9] Y. Choi and W. Szpankowski, “Compression of graphical structures: Fundamental limits, algorithms, and experiments,” *IEEE Trans. Inf. Theory*, vol. 58, no. 2, pp. 620–638, 2012.

[10] J.-L. Lu, F. Valois, M. Dohler, and D. Barthel, “Quantifying organization by means of entropy,” *IEEE Commun. Lett.*, vol. 12, no. 3, pp. 185–187, 2008.

[11] J. P. Coon, “Topological uncertainty in wireless networks,” in *2016 IEEE Global Communications Conference (GLOBECOM)*. IEEE, 2016, p. to appear.

[12] X. Zhou, S. Durrani, and H. M. Jones, “Connectivity analysis of wireless ad hoc networks with beamforming,” *IEEE Trans. Veh. Technol.*, vol. 58, no. 9, pp. 5247–5257, 2009.

[13] S.-J. Tu and E. Fischbach, “Random distance distribution for spherical objects: general theory and applications to physics,” *Journal of Physics A: Mathematical and General*, vol. 35, no. 31, p. 6557, 2002.

[14] Z. Khalid and S. Durrani, “Distance distributions in regular polygons,” *IEEE Trans. Veh. Technol.*, vol. 62, no. 5, pp. 2363–2368, 2013.

[15] S. N. Chiu, D. Stoyan, W. S. Kendall, and J. Mecke, *Stochastic Geometry and Its Applications*. John Wiley & Sons, 2013.

[16] F. Hansen and F. I. Meno, “Mobile fading - Rayleigh and lognormal superimposed,” *IEEE Trans. Veh. Technol.*, vol. 4, no. 26, pp. 332–335, 1977.

[17] H. Suzuki, “A statistical model for urban radio propagation,” *IEEE Trans. Commun.*, vol. 25, no. 7, pp. 673–680, 1977.

[18] A. Abdi and M. Kaveh, “K distribution: an appropriate substitute for Rayleigh-lognormal distribution in fading-shadowing wireless channels,” *Electronics Letters*, vol. 34, no. 9, pp. 851–851, 1998.

[19] S. Al-Ahmadi and H. Yanikomeroglu, “On the approximation of the generalized-K distribution by a gamma distribution for modeling composite fading channels,” *IEEE Trans. Wireless Commun.*, vol. 9, no. 2, pp. 706–713, 2010.

[20] F. Graziosi and F. Santucci, “On SIR fade statistics in Rayleigh-lognormal channels,” in *Communications, 2002. ICC 2002. IEEE International Conference on*, vol. 3. IEEE, 2002, pp. 1352–1357.

[21] “NIST Digital Library of Mathematical Functions,” <http://dlmf.nist.gov/>, Release 1.0.13 of 2016-09-16, f. W. J. Olver, A. B. Olde Daalhuis, D. W. Lozier, B. I. Schneider, R. F. Boisvert, C. W. Clark, B. R. Miller and B. V. Saunders, eds. [Online]. Available: <http://dlmf.nist.gov/>

[22] A. Goldsmith, *Wireless Communications*. Cambridge University Press, 2005.